



# Effects of basal forebrain stimulation on the vibrotactile responses of neurons from the hindpaw representation in the rat S1 cortex

Bige Vardar<sup>1</sup> · Burak Güçlü<sup>1</sup>

Received: 2 August 2019 / Accepted: 13 May 2020 / Published online: 3 June 2020  
© Springer-Verlag GmbH Germany, part of Springer Nature 2020

## Abstract

Basal forebrain (BF) cholinergic system is important for attention and modulates sensory processing. We focused on the hindpaw representation in rat primary somatosensory cortex (S1), which receives inputs related to mechanoreceptors identical to those in human glabrous skin. Spike data were recorded from S1 tactile neurons ( $n = 87$ ) with (ON condition: 0.5-ms bipolar current pulses at 100 Hz; amplitude 50  $\mu$ A, duration 0.5 s at each trial) and without (OFF condition) electrical stimulation of BF in anesthetized rats. We expected that prior activation of BF would induce changes in the vibrotactile responses of neurons during sinusoidal (5, 40, and 250 Hz) mechanical stimulation of the glabrous skin. The experiment consisted of sequential OFF–ON conditions in two-time blocks separated by 30 min to test possible remaining effects. Average firing rates (AFRs) and vector strengths of spike phases (VS) were analyzed for different neuron types [regular spiking (RS) and fast spiking (FS)] in different cortical layers (III–VI). Immediate effect of BF activation was only significant by increasing synchronization to 5-Hz vibrotactile stimulus within the second block. Regardless of frequency, ON–OFF paired VS differences were significantly higher in the second block compared to the first, more prominent for RS neurons, and in general for neurons in layers III and VI. No such effects could be found on AFRs. The results suggest that cholinergic activation induces some changes in the hindpaw area, enabling relatively higher increases in synchronization to vibrotactile inputs with subsequent BF modulation. In addition, this modulation depends on neuron type and layer, which may be related to detailed projection pattern from BF.

**Keywords** Attention · Touch · Somatosensory cortex · Cholinergic system · Deep brain stimulation · Synchronization · Microinjection

## Introduction

Sensory processing in the cortex is known to be modulated by intrinsic dynamics of cortical networks (Tsodyks et al. 1999; Fiser et al. 2004; Poulet and Petersen 2008) and specialized neuromodulatory circuits (e.g., the cholinergic system), which are essential for regulating the behavioral state of the animal. The cholinergic system contributes to sensory and cognitive functions as shown in numerous behavioral studies with rats (Himmelheber et al. 2000, 2001; Oldford and Castro-Alamancos 2003; Levin et al. 2006) and primates

(Hyvärinen et al. 1980; Poranen and Hyvärinen 1982; Hsiao et al. 1993; Burton et al. 1997; Steinmetz et al. 2000). Many sensory modalities are involved (auditory: McKenna et al. 1988, visual: Sillito and Kemp 1983; Sato et al. 1987, somatic: Donoghue and Carroll 1987; Dykes and Lamour 1988; Lamour et al. 1988; Metherate et al. 1988; Tremblay et al. 1990a, b), as well as functions such as learning, memory (Himmelheber et al. 2001), attention (Perry et al. 1999; Klinkenberg et al. 2011), and cortical plasticity in general (Verdier and Dykes 2001).

Abilities requiring attentional demands (e.g., responding to cues, signals, or targets) are affected when cholinergic input to the associated cortex is blocked (Torres et al. 1994; Herremans et al. 1996; Herrero et al. 2008). In particular, the basal forebrain (BF) cholinergic system originating from the nucleus basalis magnocellularis of Meynert (NB) projects diffusely throughout the neocortex (Záborszky et al. 2012, 2015), and it has been implicated in arousal,

✉ Burak Güçlü  
burak.guclu@boun.edu.tr  
Bige Vardar  
bigevardar88@hotmail.com

<sup>1</sup> Institute of Biomedical Engineering, Boğaziçi University, Kandilli Campus, Çengelköy, 34684 Istanbul, Turkey

attention (Hasselmo et al. 1995; Everitt and Robbins 1997; Sarter et al. 2005), sensory-coding (Goard and Dan 2009), motivation, memory, and experience-dependent cortical plasticity (Kilgard and Merzenich 1998; Froemke et al. 2007; Picciotto et al. 2012; Ballinger et al. 2016). There is still an ongoing effort in the literature to specify which cortical regions are essential for attention, and the current understanding of attentional mechanisms lacks considerable knowledge regarding the tactile modality. The effects of tactile attention on behavior are generally assumed to be mediated by increased neuronal firing rates and/or synchronized spikes during a tactile task (Hsiao et al. 1993; Steinmetz et al. 2000). However, the neural mechanisms based on cholinergic inputs, which maintain the control of attention in the related cortical areas for a given task, are not well known. According to the proposed model by Sarter et al. (2005), attention may be influenced by the cholinergic system through two distinct, but overlapping/interacting neural mechanisms. One mechanism is the ‘signal-driven modulation of detection’ which might be only mediated by the external signals via the sensory systems (bottom-up), whereas the other mechanism (top-down) may be mediated by practice or experience via the prefrontal modulation of the cholinergic system. Since both suggested mechanisms require the activation of BF circuits, NB seems to be important for the dynamic modulation of sensory processing.

Although considerable anatomical and pharmacological evidence exist suggesting that acetylcholine (ACh) is a neuromodulatory neurotransmitter in primary sensory cortices, its exact role in sensory processing remains unknown. For example, studies on the somatosensory cortex of both rats (Donoghue and Carroll 1987; Lamour et al. 1988) and cats (Metherate et al. 1987, 1988) have shown that ACh can modify the response to sensory inputs. It was consistently found in these studies that pairing ACh with a somatosensory input results in an increased response to the somatosensory input; this usually occurred without an increase in the baseline activity of the neuron. A variety of changes in the response to sensory input were noted in different cells, for example an increase in the receptive field (RF) size, a decrease in threshold and/or a stronger response to constant stimuli. However, none of these studies analyzed the response properties of the cortical neurons in the same detail as for visual cortex (Pinto et al. 2013; Mincec et al. 2017), such a concept of improved signal-to-noise ratio has not been fully established in the tactile modality (Oldford and Castro-Alamancos 2003). On the other hand, apart from the studies investigating the immediate effects, ACh has also long-lasting facilitatory effect on the responses of cortical neurons. This behavior has been described in a variety of studies with different species (cat, rat, and racoon) and cortical areas (somatosensory, auditory, and visual) in both in vivo and in vitro experiments (Metherate et al. 1987, 1988; Lamour et al. 1988; Tremblay et al.

1990a, b; Lin and Phillis 1991; Metherate and Ashe 1991). These experiments have differed in the type of cholinergic input to produce this enhancement in the way that ACh have been applied (iontophoretically or indirectly by electrical stimulation of BF), and in the type of response being measured (single unit activity or population responses).

There are numerous studies about peripheral sensory mechanisms involved in transducing the tactile stimuli (Talbot et al. 1968; Johansson et al. 1982; McKenna et al. 1988; Leem et al. 1993; Goodwin et al. 1995; Harris et al. 1999; Vega-Bermudez and Johnson 1999; Güçlü and Bolanowski 2003a, b, 2004; Devocioğlu and Güçlü 2013). However, the neural mechanisms involved in processing of tactile information in the skin-related areas of rat primary somatosensory cortex (S1) are not well understood in contrast to the barrel field which has a distinct cytoarchitecture (Welker and Woolsey 1974; Simons 1978; Kyriazi and Simons 1993; Dykes and Lamour 1988; Pinto et al. 2000; Foffani et al. 2004; Tutunculer et al. 2006). In each cortical column, thalamocortical inputs make synapse first in layer IV where the signal projects to upper layers of the cortex (layer II/III). Lastly, these signals pass to layer V and VI where the signal is transmitted to other areas of the brain or back to thalamus (Chapin 1986; Chapin et al. 1987; Castro-Alamancos et al. 2002; Castro-Alamancos 2004). We previously reported that cortical responses in the hindpaw representation of S1 are dependent on the frequency of tactile stimuli and cortical layer (Vardar and Güçlü 2017). Responses to 40 and 250 Hz stimuli were quickly suppressed in single neurons as opposed to those to 5 Hz stimuli, which also generated appreciable entrainment. This particular S1 area is important, because it receives inputs related to mechanoreceptors identical to those in primates including the human glabrous skin (Güçlü et al. 2003, 2008).

S1 cortex, and presumably the hindpaw area, receives cholinergic innervation mainly from neurons located at NB in BF (Mesulam et al. 1983; Semba 2000). Microiontophoresis of ACh and stimulation of NB induced long-lasting modifications of neuronal responses that were also present during wakefulness (Metherate et al. 1988; Tremblay et al. 1990a, b; Verdier and Dykes 2001; Oldford and Castro-Alamancos 2003; Constantinople and Bruno 2011). To have better understanding of the modulation caused by cholinergic activation in the rat S1 cortex, we electrically stimulated the BF, and investigated both immediate and remaining effects by single-unit recordings in the hindpaw area. Specifically, we calculated the changes in vibrotactile responses of distinct cell types (RS: regular-spiking, FS: fast-spiking) from different layers. Immediate and remaining effects of BF stimulation were analyzed on the average firing rate (AFR) calculated for three periods; before mechanical stimulus, onset period (initial 100-ms of stimulus), and remaining portion (400 ms) of vibrotactile stimulus applied

at different frequencies (5, 40, and 250 Hz). Furthermore, vector strength (VS) was calculated to quantify synchronization with respect to the periodic stimulus.

VS measure allows one to track information transmission along neural pathways. For example, higher VS in a given cortical layer and at a particular frequency may imply better spatiotemporal tuning. It was hypothesized that BF stimulation, i.e., cholinergic activation, may induce such effects, somewhat mimicking the top-down attentional influence. In other words, higher synchronization may be the substrate for higher attentional focus on the periodic stimulus. The current study is novel that spike activity in the hindpaw area of S1 cortex was analyzed with respect to well-controlled vibrotactile stimuli. Therefore, immediate and remaining effects of BF stimulation could be evaluated based on subtle changes in the response properties of RS and FS neurons in different cortical layers. The major finding of the study is that repetitive BF stimulation causes presumably some plastic changes in S1 hindpaw area neurons, which increase their synchronization to low frequency vibrotactile inputs when cholinergic activation is later retriggered. Since tactile inputs experienced in the nature can be considered to be the sum of many vibratory components, cholinergic modulation of tactile neurons seems to enhance only the low-frequency responses. This work may guide subsequent studies, especially those focusing on local circuitry related to somatosensory attention, in this particular cortical area of the rat with sensory inputs similar to those in humans. Preliminary results were presented as a conference abstract (Vardar and Güçlü 2018).

## Materials and methods

### Animals and surgery

All experiments were approved by the Boğaziçi University Institutional Ethics Committee for the Local Use of Animals in Experiments. Twenty-four adult Wistar albino rats (12 females, 12 males, weight range: 183–470 g) were used. Rats were maintained in cages housed in a climate-controlled room on 12:12-h light–dark cycles. For surgery, rats were anesthetized with ketamine (65 mg/kg) and xylazine (10 mg/kg) intraperitoneally (IP). Rectal temperature was monitored and kept at 37 °C by a heating pad (TCAT-2LV; Physitemp Instruments, Clifton, NJ, USA). The general condition of the rat was checked periodically as well as the state of anesthesia by testing palpebral and pedal reflexes. To maintain the appropriate level of anesthesia, additional anesthetic with 1/3 of induction dose was administered. To prevent brain edema and to decrease intracranial pressure, furosemide (2 mg/kg), and mannitol (0.2 g/kg) were injected IP. Additionally, atropine (0.05 mg/kg) was given IP before

the surgery to decrease bronchial secretions. Lactated Ringer solution (40 ml/kg/24 h, IP) was given to maintain normal physiological conditions for longer experimental durations. The head was fixed to a stereotaxic frame, and the craniotomy was performed over the hindpaw representation of S1 and electrode insertion axis of NB (Chapin and Lin 1984; Paxinos and Watson 1997). Custom-made bipolar tungsten stimulating electrodes (World Precision Instruments, Sarasota, FL, USA) were implanted in the left NB and fixed to the skull along with a plastic recording chamber over SI using dental acrylic. After recordings, the rat was either euthanized with an overdose of thiopental (200 mg/kg, IP) or perfused transcardially for a subsequent histology study.

### Single-unit recording and vibrotactile stimulation

Single-unit action potentials (spikes) were recorded through a carbon fiber electrode (Carbostar-6; Kation Scientific, Minneapolis, MN, USA). All recordings were done in a Faraday cage ( $1.58 \times 1.05 \times 1.20 \text{ m}^3$ ). RFs in the hindpaw representation were mapped by using von Frey (VF) hairs. The recording electrode was positioned by a hydraulic microdrive (MHW-4; Narishige International, London, UK). Spikes were amplified by a custom-made microelectrode amplifier (gain 1000; pass band 200 Hz–10 kHz). Single units were isolated with an amplitude window discriminator (model 121; World Precision Instruments, Sarasota, FL, USA). Neural activity was visualized and heard by an oscilloscope and a speaker, respectively. All data including raw voltage traces and discriminated spikes were collected in a PC through a custom-made MATLAB (Version R2008a; The MathWorks, Natick, MA, USA) program and a data-acquisition card (USB-6251; National Instruments, Austin, TX, USA) with a sampling rate of 100 kHz.

Mechanical vibrotactile stimuli were generated by an analog output of the USB-6251 card. The waveforms were level-adjusted by a digital attenuator (model V2.0C; ISR Instruments, Syracuse, NY, USA) and amplified by a custom-made power amplifier to drive an electrodynamic shaker (V201; Ling Dynamic Systems, Royston, Herts, UK). The vibrotactile stimuli were applied at the RF center of each single unit at the contralateral side by using a plastic cylindrical contactor probe (diameter 1.8 mm) connected to the shaker. They were presented as bursts of sinusoidal mechanical vibrations (amplitude 100  $\mu\text{m}$  peak-to-peak, duration 0.5 s) upon 0.5-mm static indentation to prevent decoupling from the skin (Cohen et al. 1999; Devocioğlu and Güçlü 2013). The sinusoidal frequencies were 5, 40, 250 Hz, and the waveforms started and ended as cosine-squared ramps with 50-ms rise/fall times. Displacements of the contactor probe were calibrated by using Fotonic sensor (MTI-2100; MTI Instruments, Albany, NY, USA).

## Electrical BF stimulation

Electrical BF stimulation was applied at NB (ML + 2.4 mm, AP – 1.3 mm, DV + 6.8 mm; Paxinos and Watson 1997; Gourd and Dan 2009) while recording from the hindpaw area of S1 in the same hemisphere (see “Discussion” for contralateral data). Since the dorsoventral axis from NB overlaps with S1 cortex, the stimulation electrodes were inserted with an angle of 20° at a location on the skull (ML + 2.4 mm; AP – 3.78) not to damage the recording area. Coordinates were normalized according to bregma-lambda distance of each animal. Electrical stimulation consisted of biphasic charge-balanced current pulses (pulse duration 0.5 ms) with amplitude of 50  $\mu$ A, and they were applied 50 times (0.5 s at 100 Hz) at each trial. Long-term monophasic stimulation may cause tissue damage due to charge accumulation and slow Faradaic currents; therefore, biphasic waveforms are typically preferred in neurostimulation applications (Merrill et al. 2005). Figure 1 shows the experimental protocol and the timing diagram of electrical BF stimulation and vibrotactile stimulation of the skin. The total number of pulses in each time block is 1500 (50 pulses per trial  $\times$  10 trials for each frequency  $\times$  3 different vibrotactile frequencies).

We also performed preliminary experiments (i.e., 20 neurons) with microinjection of ACh (100  $\mu$ M) and two nicotinic receptor antagonists in the hindpaw area of S1 cortex:

methyllycaconitine (MLA) ( $\alpha$ 7 nicotinic receptor antagonist; 0.5  $\mu$ M), and dihydro- $\beta$ -erythroidine-hydrobromide (Dh $\beta$ E) (non- $\alpha$ 7 nicotinic receptor antagonist; 10  $\mu$ M). These drugs were applied with 20-ms pressure pulses 5 times at each trial (inter-pulse interval 0.1 s) just before the BF stimulation period only for 5-Hz vibrotactile stimulation. Each pulse approximately yielded 8 nL of a drug solution (for details on instrumentation, see Vardar and Güçlü 2017).

## Experimental procedure

Each single unit recording from S1 consisted of two blocks, and both blocks included three different vibrotactile stimuli (5, 40, and 250 Hz) under control (OFF) and BF stimulation conditions (ON) (Fig. 1a). The vibrotactile stimulus was repeated for 10 trials at each OFF and ON condition (one trial duration 2 s, intertrial interval 3 s). The OFF conditions did not have BF stimulation; in the ON conditions, electrical current pulses were applied just before the vibrotactile stimulus started in a trial (Fig. 1b). Blocks were separated with 30 min time interval to study the remaining effects of cholinergic activation. There were also 10 min time intervals between different frequency conditions to ensure that the immediate effects of BF had diminished. The sequence of conditions was ordered to study the effects of time blocks statistically. Previously, we showed that the vibrotactile responses stay stable for such durations if no BF activation is applied (Vardar and Güçlü 2017). However, since there is repetitive BF stimulation in the current study, we specifically compared the baseline (i.e., spontaneous) firing rate ( $R_b$ , see “Results” below) across conditions and verified that it stays constant.

## Neuron classification and data analysis

Neurons were classified from single-unit data according to RF maps, VF thresholds, recording depths, and spike shape. RF type and cortical layer classes were determined according to the previous literature (for details, see Chapin 1986; Dykes and Lamour 1988; Güçlü 2013; Vardar and Güçlü 2017). The main criterion for the RF types was the inclusion of digits; nine different letter categories were defined (Güçlü 2013): (A) single digit, (B) multiple digits, (C) only pad(s), (D) digit(s), and pad(s), (E) upper paw without digits, (F) lower paw, (G) digit(s), pad(s), and neighboring sole, (H) entire paw without digits, (I) entire paw. In addition, neurons were classified as regular spiking (RS), fast spiking (FS), and intrinsically bursting (IB) based on their spike shapes and firing pattern (Mountcastle et al. 1969; Simons 1978; Connors and Gutnick 1990) by analyzing raw voltage traces. The spike waveforms were plotted and the durations were measured manually offline on the plots in MATLAB (Vardar and Güçlü 2017). Because we also had the spike

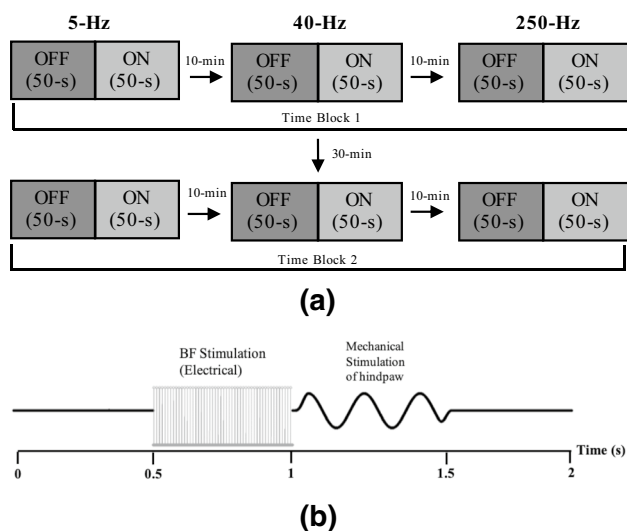


**Fig. 1** **a** Experimental procedure. Each condition (OFF: no BF stimulation, ON: BF electrical stimulation) included 10 trials and lasted 50 s. The OFF–ON sequence with the order of vibrotactile frequencies (5, 40, 250 Hz) made up a time block. 30 min after the first block, the entire sequence was repeated (second time block). Different frequency conditions were separated by 10 min. **b** Timing diagram for each trial. Each trial lasted 2 s. The BF electrical stimulation was applied between 0.5 and 1 s (only in ON conditions), and the vibrotactile stimulus was presented between 1 and 1.5 s. Inter-trial interval was 3 s

time stamps from the window discriminator output, it was simple to distinguish the relevant units. FS units are identified as having spike durations <0.5 ms. RS units have slower repolarization, so they are recognized with spike durations >0.5 ms. IB units are relatively easy to classify; their spikes occur in a clustered pattern.

Cortical depths of the neurons were estimated by using the electrode position which was set by the hydraulic microdrive with high accuracy (~ 1 μm) with respect to cortical surface. After some experiments, we inspected the tissue marking of the electrode in brain sections and confirmed its tip location based on cortical layer thicknesses obtained by Nissl staining. The cortical layer data reported here are based on the average layer boundaries calculated from our previous work (Yusufoğulları et al. 2015) and other studies (Chapin 1986; Dykes and Lamour 1988).

To visualize the rate and timing of spike discharges in response to a vibrotactile stimulus, peri-stimulus time histograms (PSTHs, bin size 50 ms) and spike-phase (SP) histograms (bin size 0.5°) were constructed. However, spike counts were used without narrow binning for statistical analyses of AFRs. For each frequency and stimulation condition (OFF–ON), spike data were pooled for 10 trials, and analyzed for changes in AFR and VS. AFRs were calculated for different time periods: before stimulus ( $R_b$ ), onset period ( $R_o$ ) (first 100-ms of stimulus), and last 400 ms of vibrotactile stimulus ( $R_{d*}$ ). To quantitatively compare the response of a neuron to mechanical stimulation, background activity ( $R_b$ ) was subtracted from  $R_o$  and  $R_{d*}$  for each tested frequency.

Since the vibrotactile stimulus used in this study has a simple waveform (i.e., sinusoidal burst), a synchronization measure such as the vector strength is adequate and has frequently been used before (e.g., Whitsel et al. 2000; Grün and Rotter 2010). Vector strength shows how the spike times are aligned with respect to the successive cycles of the stimulus. Each spike is considered as a unit vector with an angle ( $\theta_i$ ) ranging from 0 to  $2\pi$ . This angle is calculated as  $\theta_i = (2\pi t_i)/T$ , where  $t_i$  is relative spike time with respect to stimulus cycle onset and  $T$  is the period of the vibrotactile stimulus. For a set of  $n$  unit vectors with angles ( $\theta_1, \theta_2, \dots, \theta_n$ ), the rectangular coordinates ( $x, y$ ) of the vector sum can be written as:

$$(x, y) = \left( \sum_{i=1}^n x_i, \sum_{i=1}^n y_i \right) = \left( \sum_{i=1}^n \cos \theta_i, \sum_{i=1}^n \sin \theta_i \right). \tag{1}$$

The magnitude ( $r$ ) of the vector sum is:

$$r = \sqrt{x^2 + y^2} = \sqrt{\left( \sum_{i=1}^n \cos \theta_i \right)^2 + \left( \sum_{i=1}^n \sin \theta_i \right)^2}. \tag{2}$$

Therefore, VS is derived from this resultant vector’s magnitude by averaging with respect to the number of spikes:

$$VS = \frac{1}{n} \sqrt{\left( \sum_{i=1}^n \cos \theta_i \right)^2 + \left( \sum_{i=1}^n \sin \theta_i \right)^2}. \tag{3}$$

VS has a range of 0–1, where 1 implies perfect synchronization such that all unit vectors are unidirectional, i.e., spikes occur regularly with the same period as the stimulus. VS is 0 when spike times are randomly distributed within stimulus cycles.

Most of the analyses were performed in MATLAB R2016b and MS Excel. For statistical testing, repeated measures ANOVA and was done in SPSS Ver.23 (IBM Corp., Armonk, NY, USA) in which the vibrotactile frequency, OFF vs. ON conditions, and time block were within-subject (-neuron) factors, while cortical layer and neuron type (RS vs. FS) were between-subject (-neuron) factors. Post hoc analyses were also done in SPSS if a factor was found significant. IB neurons were not included in the statistical analyses, because their sample size was small. In addition, no significant subject gender differences were found, so this result was not reiterated in the analyses below.

## Results

### Classification of vibrotactile neurons

Recordings were obtained from a total of 87 neurons in the hindpaw representation of S1 cortex. Neurons were sampled from layer III ( $n = 10$ ), IV ( $n = 33$ ), V ( $n = 35$ ) and VI ( $n = 9$ ) (Table 1). They mostly had medium VF thresholds (84%) and those were usually sampled from layer IV ( $n = 24$ ) and V ( $n = 31$ ). Those who had low VF thresholds (16%) were mostly found in layer IV ( $n = 9$ ). There were no neurons recorded with high VF thresholds (> 2.5 g). The RFs largely varied throughout the cortex and across neurons as reported previously (Güçlü 2013; Vardar and Güçlü 2017), but the most common RF type was D (28%) which included a single digit and pads near the digit. Type E (13%) and type G (16%) were also found frequently; they included an area covering the upper paw (without digits) and single/multiple digits with pads, respectively.

In addition, the neurons were classified as RS ( $n = 42$ ), FS ( $n = 31$ ), and IB ( $n = 14$ ) based on spike shape. RS and FS neurons were mostly found in layers IV and V, consistent with the relatively larger sample size in these layers. No neurons were sampled from layers I and II in this study. On the other hand, RS neurons typically had RF types of D, F, and G; they covered a single digit and pad(s) or lower paw. For FS neurons, RF types D and G were

**Table 1** Classification of vibrotactile neurons in the hindpaw representation of SI cortex

	Cortical layers						Receptive field classification						Total	
	III	IV	V	VI	A	B	C	D	E	F	G	H		I
<i>von Frey thresholds</i>														
Low (<0.25 g)	1	9	4	0	0	2	0	5	1	1	3	0	2	14 (16%)
Medium (0.25–2.5 g)	9	24	31	9	6	7	3	19	10	7	11	5	5	73 (84%)
<i>Type of Neuron</i>														
Regular spiking (RS)	6	18	15	3	4	4	1	10	3	6	6	5	3	42 (48%)
Fast spiking (FS)	2	10	15	4	1	5	2	10	4	2	6	0	1	31 (36%)
Intrinsically bursting (IB)	2	5	5	2	1	0	0	4	4	0	2	0	3	14 (16%)
<i>Cortical layers</i>														
III					1	0	0	3	0	1	2	2	1	10 (11%)
IV					4	3	2	8	3	4	5	1	3	33 (38%)
V					1	3	1	9	8	2	7	2	2	35 (40%)
VI					0	3	0	4	0	1	0	0	1	9 (11%)
Total	10 (11%)	33 (38%)	35 (40%)	9 (11%)	6 (6%)	9 (11%)	3 (3%)	24 (28%)	11 (13%)	8 (9%)	14 (16%)	5 (6%)	7 (8%)	87

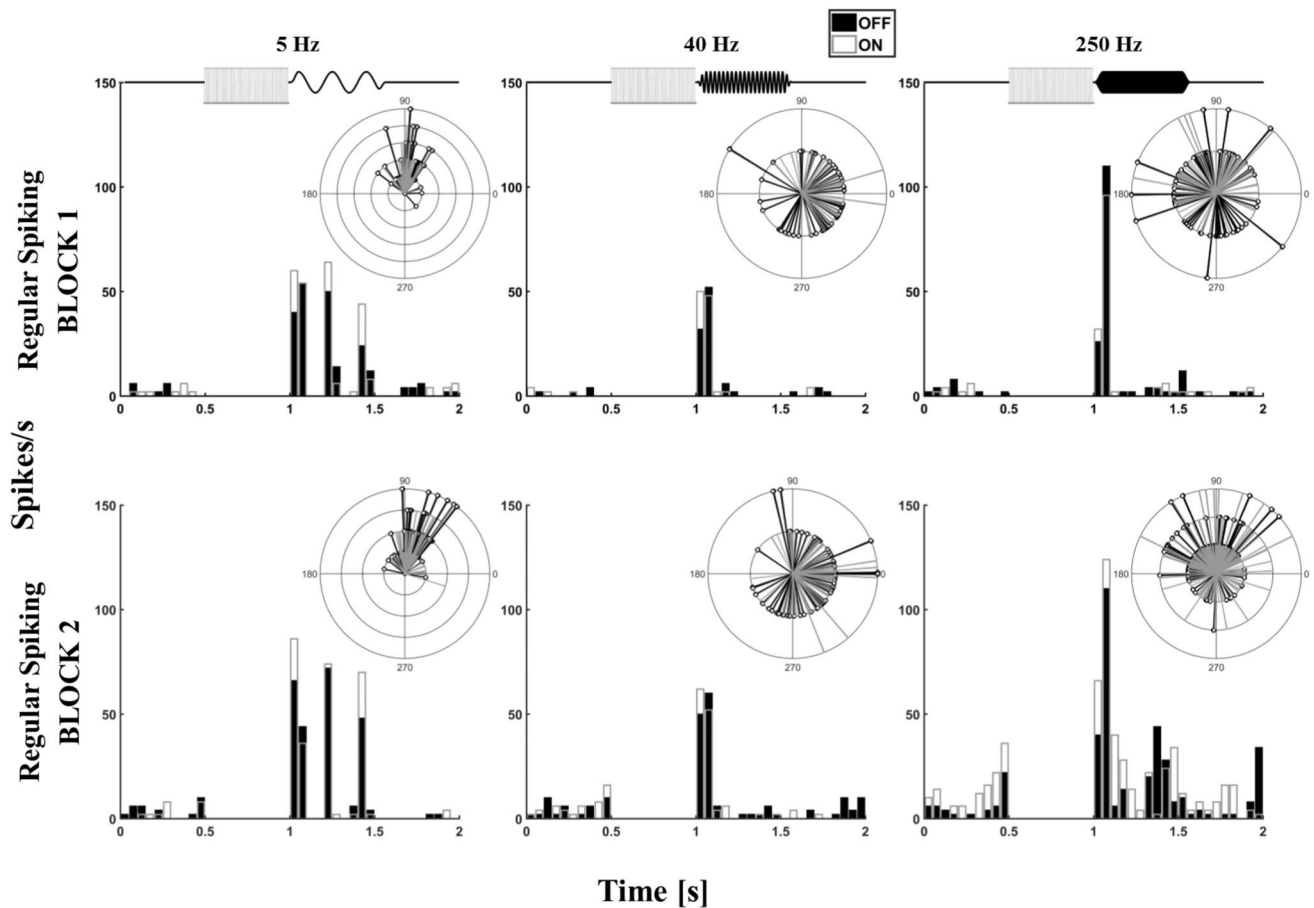


**Fig. 2** Peristimulus time histograms (PSTHs) and spike-phase (SP) histograms of a regular spiking neuron for first and second time blocks. The vibrotactile displacement waveforms are given above the PSTHs and share the same time axes (left 5 Hz, middle 40 Hz, right 250 Hz). BF stimulation preceded the vibrotactile stimuli; spike recording was blanked between 0.5 and 1 s due to electrical artifacts.

also frequently found. IB neurons mostly had RF types D (single digit and pad) and E (upper paw without digits) consistent with the previous work (Güçlü 2013; Vardar and Güçlü 2017).

### Vibrotactile responses without BF stimulation

For qualitative comparisons, PSTHs were constructed to show neural activity for both OFF and ON conditions. The black bars in PSTHs and black vectors in SP histograms are for OFF conditions in which there was no BF stimulation. It is important to note that the histograms are blanked for the time window in which BF stimulation was presented due to the electrical stimulation artifact. For consistency, data were not analyzed in the same window for the OFF conditions as well. Figures 2 and 3 exemplify activity profiles for an RS neuron and a FS neuron, respectively. Other neurons of a given class had similar histogram plots. Consistent with the

previous literature (Güçlü 2013; Vardar and Güçlü 2017), almost all neurons had vigorous onset spikes with markedly decreased activity throughout the remaining duration of the vibrotactile stimulus at 40 and 250 Hz frequency. However, at 5 Hz, the neurons could be partially entrained, i.e., they generated spikes at each cycle of the stimulus. Thus, higher synchronicity could be observed at 5 Hz; SP histograms have vectors accumulated in a narrower range of degrees.

There was a significant neuron  $\times$  layer interaction ( $p = 0.018$ ) on the background AFR. Specifically in layer III, FS neurons have significantly higher background activity ( $15.40 \pm 3.92$  spikes/s) as compared to RS neurons ( $6.05 \pm 1.12$  spikes/s). However, in the other tested layers,  $R_b$  is similar for both RS and FS. Furthermore, because the protocol involved repetitive BF stimulation, we compared background AFR only in OFF conditions within and across the time blocks and found no significant differences. This verified that the statistical comparisons presented with BF

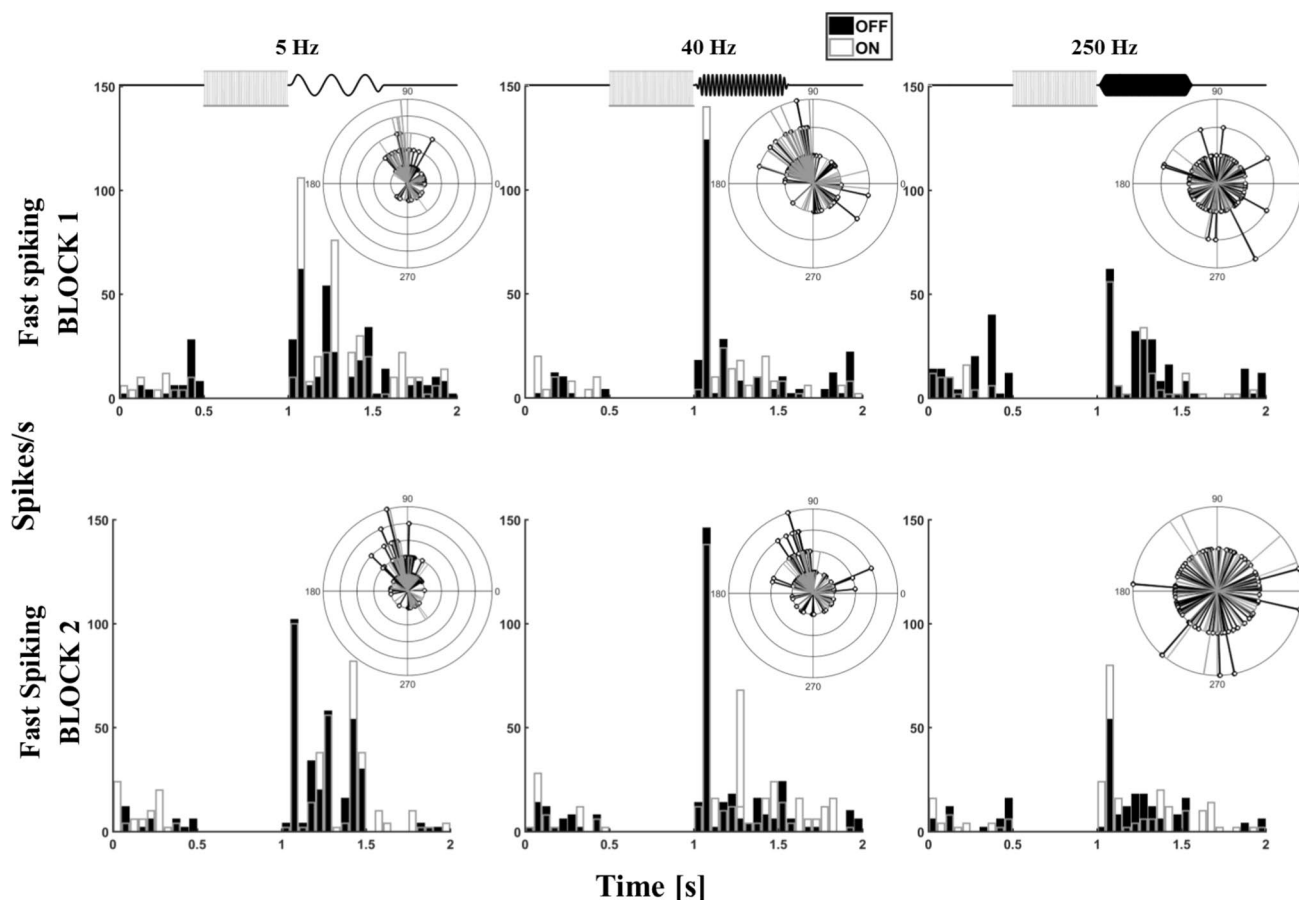


**Fig. 3** Peristimulus time histograms (PSTHs) and spike-phase (SP) histograms of a fast spiking neuron for first and second time blocks. See Fig. 2 caption for details

stimulation are valid in the sense that the background activities of the neurons were not affected. However, as presented below, there was a remaining effect on vibrotactile synchronization which could only be observed with further BF stimulation after 30 min.

To statistically assess the change in spike response due to vibrotactile stimuli in the OFF condition (with time–block data pooled), the background AFR ( $R_b$ ) was subtracted from the AFR during the initial 100-ms period of the stimulus ( $R_o$ ) and from the AFR of the remaining portion of the stimulus ( $R_d^*$ ). Statistical tests for the AFR measures and VS were done by repeated-measures ANOVA with stimulus frequency as within-subject factor, and cortical layer and neuron type (RS vs. FS) as between-subject factors. The ANOVA results show that the frequency had a main effect on  $R_d^*-R_b$  and on VS ( $p=0.035$  and  $p<0.001$ , respectively), but not on  $R_o-R_b$ . As seen in Fig. 4a,  $R_d^*-R_b$  at 5 Hz ( $7.96 \pm 1.60$  spikes/s) is significantly higher as compared to AFR change at 40 Hz ( $4.84 \pm 1.10$  spikes/s) and 250 Hz ( $4.76 \pm 0.88$  spikes/s). No other significant effects could be found.

As expected from the SP histograms, VS is significantly higher at 5 Hz ( $0.55 \pm 0.04$ ) as compared to 40 Hz ( $0.23 \pm 0.02$ ) and 250 Hz ( $0.20 \pm 0.02$ ) (Fig. 4b). Similar to AFR measures, significant main effects due to cortical layer and neuron type could not be found for VS values.

### Immediate effects of BF stimulation

Similar to OFF conditions, ON conditions were first qualitatively studied (see Figs. 2 and 3). Gray-outline white bars in PSTHs and gray vectors in SP histograms are for ON conditions. As in the OFF conditions, neurons mostly responded at the onset, but not as high for the remaining part of 40 and 250-Hz vibrotactile stimuli. At 5 Hz, however, spikes could be generated during all stimulus cycles throughout the entire duration. Therefore, gray vectors are accumulated in a narrower range, i.e., higher VS, in contrast to those for 40 and 250 Hz. Although the PSTHs for ON conditions sometimes seem to have higher bars than those from OFF conditions (e.g., 5-Hz data in Fig. 2), the data from the entire sample did not have a clear systematic trend. However, gray vectors



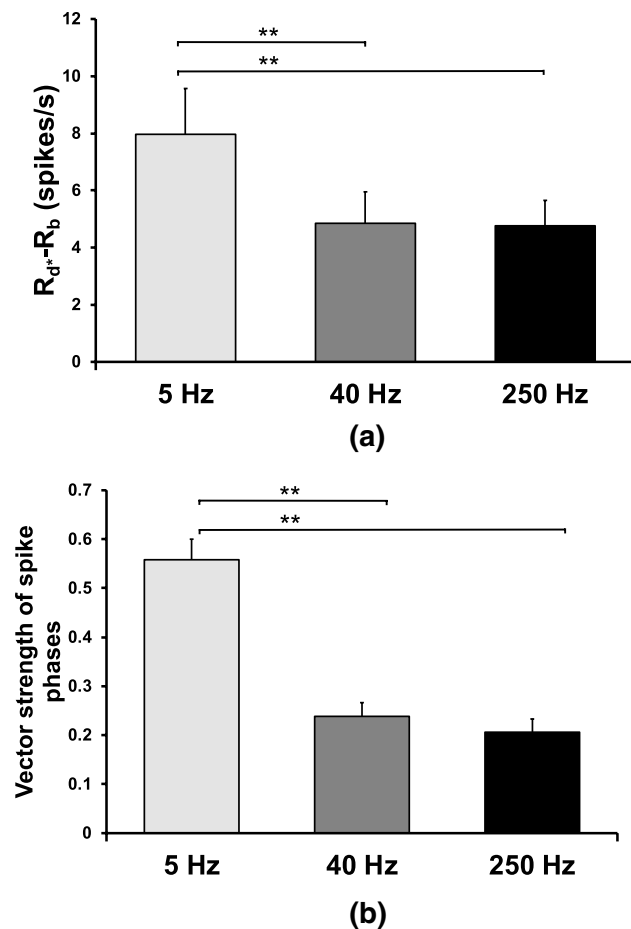


**Fig. 4** Significant differences in vibrotactile responses without BF stimulation (OFF conditions in both time blocks). **a** The average firing rate (AFR) change during the last 0.4-s portion of the vibrotactile stimulus ( $R_{d^*}-R_b$ ) for different frequencies. **b** Vector strength (VS) of spike phases referenced to vibrotactile stimulus cycles for different frequencies. Error bars are the standard errors. \* $p < 0.05$ , \*\* $p < 0.01$

were observed to be somewhat more tightly distributed than black vectors for 5-Hz vibrotactile inputs (e.g., see Fig. 3).

To analyze the immediate effects of BF stimulation statistically, activity measures in OFF and ON conditions were compared during both the first and second blocks of the protocol. Repeated measures ANOVA were performed on AFRs and VS values with stimulus frequency and OFF vs. ON conditions as within-subject factors, and cortical layer and neuron type (RS vs. FS) as between-subject factors. Although neuron type and cortical layer had some influence on the background activity, we did not find any significant changes in  $R_b$  related with BF stimulation during either the first block or the second block ( $p = 0.22$  and  $p = 0.43$ , respectively). Moreover, BF stimulation did not cause any significant immediate effects in the other AFR measures ( $R_o-R_b$ ,  $R_{d^*}-R_b$ ). In other words, the average responsiveness of the neurons to vibrotactile stimuli was not

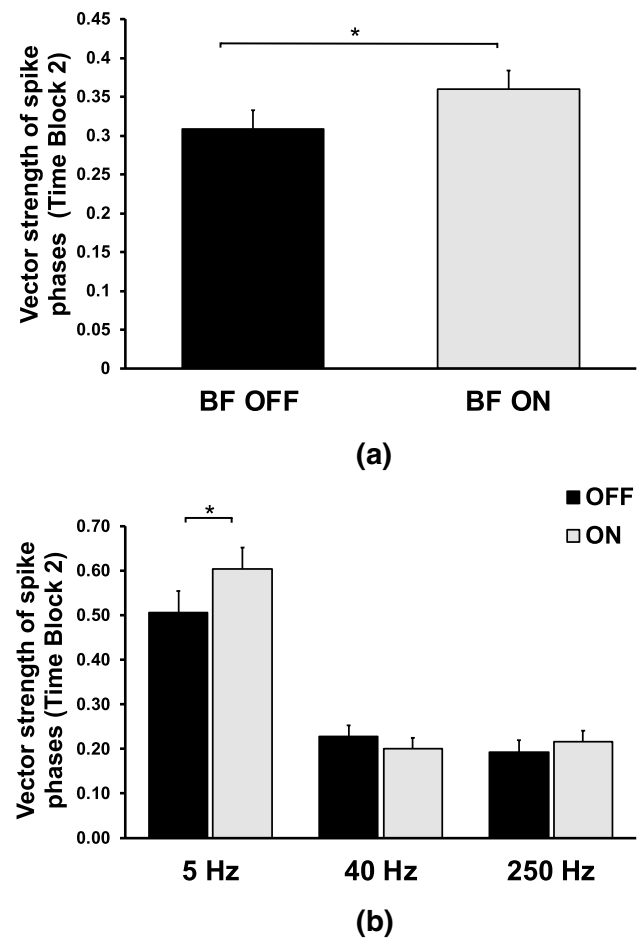


**Fig. 5** Significant differences in vibrotactile responses due to immediate effects of BF stimulation. **a** Overall effect of BF stimulation on vector strength (VS) values. **b** VS values are plotted for OFF vs. ON conditions at each vibrotactile frequency separately. Error bars are the standard errors. \* $p < 0.05$ , \*\* $p < 0.01$

affected by BF stimulation in the short term. Frequency had a similar main effect on  $R_{d^*}-R_b$  as described in the previous section.

On the other hand, frequency and BF stimulation had significant immediate effects ( $p < 0.001$  and  $p = 0.002$ , respectively) on VS values during only the second block (Fig. 5a). BF stimulation significantly increased the VS values with an interaction with vibrotactile frequency ( $p = 0.002$ ). Post hoc analyses showed that this increase was only present at 5 Hz, but not at 40 and 250 Hz (Fig. 5b). This result implies that after repetitive cholinergic activation performed during the first block, synchronicity to a low frequency vibrotactile stimulus may be increased by subsequent BF stimulation performed much later.

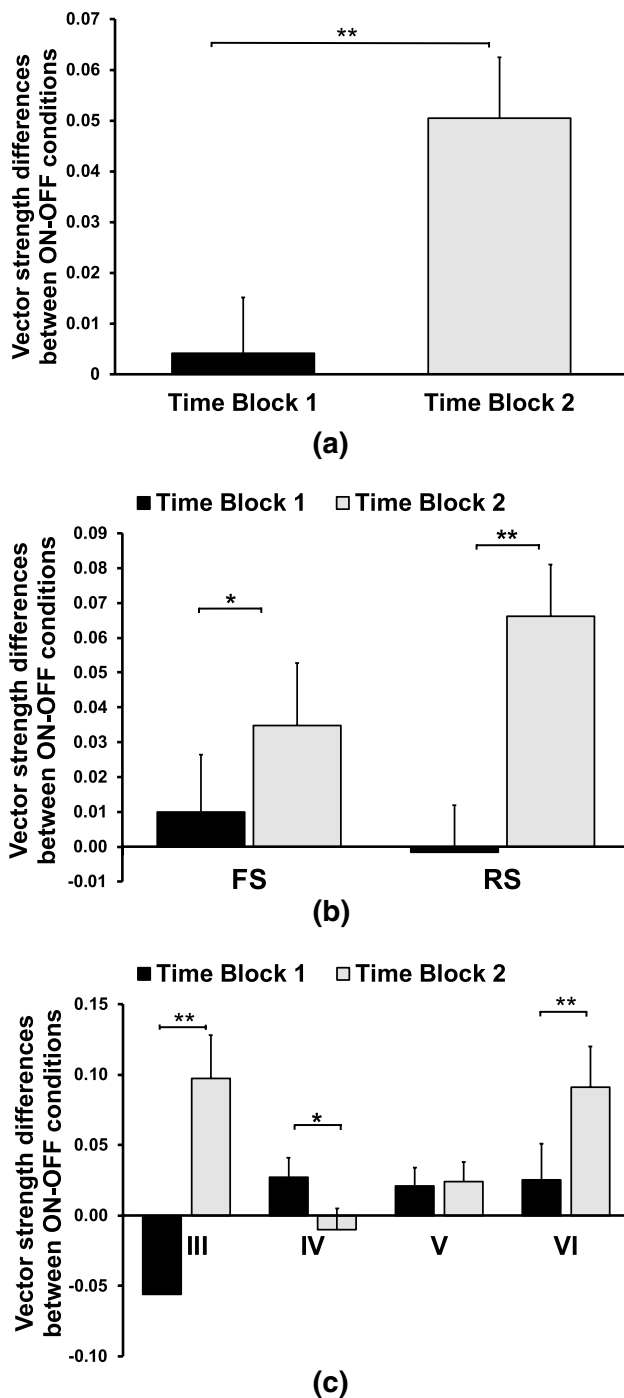


**Fig. 6** Significant differences in vibrotactile responses due to remaining effects of BF stimulation. Vector strength (VS) differences were calculated between ON–OFF conditions; positive direction indicates higher VS in ON condition. **a** Overall VS changes in different time blocks. **b** VS changes depending on FS and RS neurons (see text) in different time blocks. **c** VS changes depending on cortical layers (see text) in different time blocks. Error bars are the standard errors. \* $p < 0.05$ , \*\* $p < 0.01$

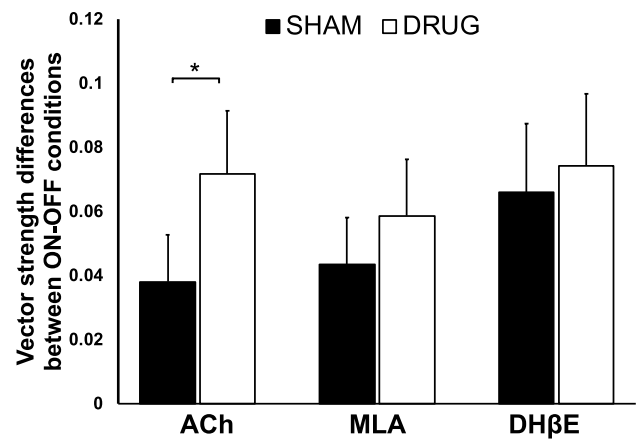


**Fig. 7** Effects of BF stimulation on VS after drug microinjection. This preliminary experiment (i.e., 20 neurons) only consisted of one frequency condition (5 Hz) and a single time block. Vector strength (VS) differences were calculated between ON–OFF conditions. Sham application was performed with artificial cerebrospinal fluid. MLA and DhβE are nicotinic receptor antagonists

### Remaining effects of BF stimulation

The results in the previous section suggest that there may be remaining effects of BF stimulation. Although there was no difference between OFF and ON conditions in the first block, there was a significant difference of VS in the second block. To understand the remaining effects explicitly, OFF and ON conditions were separately studied between the first and second blocks. Repeated-measures ANOVA was performed on AFR measures and VS values with stimulus frequency and time block (first vs. second) as within-subject factors, and cortical layer and neuron type (RS vs. FS) as between-subject factors. In a third analysis, the change in the activity measures (AFRs and VS values) were calculated within each time block from OFF to ON conditions. Then, these differences were used as dependent variables in a similar repeated-measures ANOVA.

When comparing the activity measures in OFF and ON conditions (separately) for the influence of time block did not yield significant results in AFR measures except a complex interaction (time block  $\times$  neuron type  $\times$  layer) effect on  $R_{d^*} - R_b$  for the ON conditions ( $p = 0.022$ ). Post hoc analyses showed that FS neurons in layer III were not much responsive to vibrotactile stimulation after the onset period ( $R_{d^*} - R_b \approx 0$ ) during ON conditions in both time blocks. However, FS neurons in the other layers and all RS neurons had much more activity during the stimulation period. Similar to AFR results, time block did not influence VS values in respective ON conditions and OFF conditions. There were main effects of frequency on  $R_{d^*} - R_b$  and VS similar to those in Fig. 4a, b.

Most importantly, the changes in VS due to BF stimulation was significantly affected by time. Specifically, the increase in VS was much higher in the second block compared to the first block ( $p=0.003$ , Fig. 6a). However, there were also interactions between time block  $\times$  neuron type and between time block  $\times$  layer ( $p=0.05$  and  $p < 0.001$ , respectively). The change in the VS increase due to time block was much more prominent for RS neurons (Fig. 6b). Time block had more effects on VS changes of neurons in layers III and VI (Fig. 6c). Interestingly, in layer III, BF stimulation decreased VS in the first block, but increased VS in the second block. There were no significant effects in the changes of AFR measures. Since the differences in the activity measures were analyzed in this final set of analyses, the main effect of frequency disappeared.

### Microinjection of cholinergic drugs

The preliminary microinjection data (Fig. 7) show that ACh ( $p=0.023$ ) caused an increase in the VS difference between the ON–OFF conditions with respect to sham (artificial cerebrospinal fluid) application. Therefore, the immediate synchronization effects of BF stimulation to 5-Hz vibrotactile stimulation were enhanced with ACh, but nicotinic receptor antagonists did not alter synchronization significantly within this preliminary data set. We will study the combined effect of drug microinjection and BF stimulation also on firing rates as more data accumulate. These preliminary results are currently along the same line with our previous study with atropine, but without BF stimulation (Vardar and Güçlü 2016). Consistent with the literature, that study showed vibrotactile responses depend on muscarinic receptors in deeper layers, while the spontaneous activity is increased by ACh application more in supragranular layers. It may be; therefore, conjectured that BF activation in the current study primarily acted through the muscarinic receptors and had a slowly developing neuromodulatory influence on cortical sensory processing as displayed by increased synchronization, especially at 5 Hz.

### Discussion

Among its numerous effects in cognitive function, the cholinergic system originating from BF has a modulatory influence on sensory processing. ACh release in sensory cortices enhances stimulus-evoked responses, modifies selectivity and leads to long-lasting increase in cortical excitability. It was previously shown that electrical stimulation of BF, i.e., artificial activation of the cholinergic system, may produce an enhancement of somatosensory (cutaneously) evoked potentials (Rasmusson and Dykes 1988) lasting up to 4 h. This long-lasting effect is

attributed to muscarinic receptors at the level of single cortical neurons. The current results from the hindpaw area of rat S1 cortex also show remaining effects 30 min after the first block of BF activation. The vibrotactile stimulation protocol based on three different frequencies and analyses with VS allowed us to investigate synchronization of RS and FS neurons along the cortical layers. This is important regarding spatiotemporal tuning, i.e., temporal information transfer across layers. Because natural tactile stimuli consist of many frequency components, enhancement of frequency-dependent stimulus features through BF activation may be a form of top-down attentional modulation in the awake state.

Specifically, in the current study, BF stimulation had immediate effect only in the second block. VS increased for 5-Hz vibrotactile stimuli, which indicates that over time, the neurons became more prone to synchronization to low frequency inputs, shown previously to be more salient in the hindpaw area (Vardar and Güçlü 2017). Moreover, the VS increase due to BF stimulation was significantly higher in the second block mostly for RS neurons. Although there were no appreciable VS changes for this neuron class due to BF stimulation in the first block, there was a considerable change in the second block. In other words, the synchronicity increase in the hindpaw area may be attributed to mostly excitatory neurons (for the chemical identity of RS neurons, see Fox 2008).

It is also interesting to note that such changes were mostly in layers III and VI. Since layers II/III are the main processing layers in the rat S1 cortex and layer VI sends out corticothalamic outputs, vibrotactile synchronization increase due to BF stimulation may indeed be an evidence of ‘attentional’ tuning in thalamocortical loops (Ahissar et al. 2000; Porter et al. 2001; Gabernet et al. 2005). We cannot explain at this time, why layer III neurons had a decreasing synchronicity trend in the first block due to BF stimulation; this, however, was not statistically significant.

In conclusion, BF stimulation concomitant with vibrotactile inputs develops a neuromodulatory effect over time and increases the further synchronization capability of the rat S1 neurons when they are excited by the cholinergic system originating from BF. However, this finding was relevant only for low frequency sensory inputs. Consistent with the previous studies, higher frequency vibrotactile information was suppressed after the onset period. Even though thalamocortical inputs are presumed to be present (Gil and Amitai 1996; Vahle-Hinz et al. 2007), cortical information transmission after the initial 100-ms onset period is hindered at high frequency sensory stimulation due to synaptic depression and feed-forward inhibition (Vardar and Güçlü 2017). The current results additionally show that this behavior is not influenced by BF activation. It is also interesting to point out that AFRs, i.e., average spiking activity of the neurons

subject to vibrotactile inputs, were not significantly affected by BF stimulation in our study (including response adaptation (not shown) calculated as  $R_{d*}-R_o$ ). Further studies on awake animals may confirm whether this finding is because of anesthesia or particularly due to circuits in the hindpaw area of rat S1 cortex.

### Comparison with previous drug microinjection studies

Long-lasting cholinergic enhancement of neural activity by BF stimulation was reported in the literature based on somatosensory-evoked potentials and spike rates at the level of single cortical neurons in cats. (Metherate et al. 1988; Rasmusson and Dykes 1988; Tremblay et al. 1990a, b; Verdier and Dykes 2001). On the other hand, local application of ACh caused plastic changes on firing rates and receptive field sizes. These effects were blocked by muscarinic antagonists, but not influenced by nicotinic receptors, especially in deeper layers. Similarly, Martin-Cortecero and Nuñez (2014) studied the effects of ACh application on the whisker-related response adaptation of cortical neurons. They showed that application of ACh increased both spontaneous firing rate and response to whisker stimulation in both superficial and deeper layers. Changes in response adaptation was also statistically significant and atropine injection blocked the ACh effect in type 1 neurons (putative pyramidal cells).

Metherate et al. (1988) argued, as many other researchers, that concomitant neural activity was critical to produce to long-term changes in the presence of ACh. They showed that changes preferentially occurred when ACh was paired with glutamate administration or with tactile stimulation, and very rarely when ACh was given alone. Similar to this result, Sillito and Kemp (1983) studied such effects in the visual cortex, and they found a cumulative enhancement of visual responses when successive administrations of ACh were repeated before responsiveness to visual stimuli declined to the control value. In a study on awake monkeys, BF was quite active and generated action potential continuously. Specifically, it was reported that BF neurons showed phasic changes in average firing rates at specific times during the behavioral task (Richardson and DeLong 1986). Therefore, in the current study, stimulating the BF repetitively and close in time with the vibrotactile stimulation might have changed tonic background into a robust phasic activity leading possibly to persistent changes in the relevant networks.

### Other effects of BF stimulation

Although many previous studies showed excitatory effects, NB also sends GABAergic input to the cortex that may be involved in arousal/attentional modulation (Záborszky et al. 1986; Henderson et al. 2010; Záborszky et al. 2018).

Glutamatergic and peptidergic projections have also been documented (Záborszky et al. 1999; Hur and Zaborszky 2005). Our results are not contradictory to this fact, because higher synchronization may also result from inhibiting convergent inputs not related with the vibrotactile inputs. Furthermore, our lack of finding significant effects in AFR measures may be indicative of the activation of inhibitory projections as well as excitatory ones, which may balance each other. More focused BF activation, e.g., by optogenetics, may elucidate some of the issues which were out of scope in the presented work. It is known that only a third of the projections from NB is cholinergic (Henny and Jones 2008).

In this article, we explicitly present neurophysiological data from S1 hindpaw area ipsilateral to BF stimulation. Recent studies also showed contralateral projections to sensory cortices (Chaves-Coira et al. 2018a, b). These projections may cause interhemispheric modulation of vibrotactile information. To evaluate this possibility, we additionally recorded from hindpaw area contralateral to BF stimulation. For this purpose, the vibrotactile stimulus location was shifted to the other limb to make direct comparison with the current results. Preliminary data from 12 neurons (not shown) suggest that contralateral BF stimulation did not cause neuromodulatory effects in vibrotactile responses measured by AFRs and VS.

### Limitations and future directions

Another interesting finding, which somewhat supports the statements related to concomitant vibrotactile inputs above, is related to background activity, i.e., the AFR calculated within the time window before the vibrotactile stimulus was applied. Background activity was not affected by BF stimulation in the first time block, which was expected because the time window for  $R_b$  preceded the BF stimulation interval. However, apparently there were also no remaining changes in  $R_b$ , because significant results could not be found in the second time block and in the remaining statistical analyses which focused on the differences between the time blocks. It is important to note that this does not directly imply that cholinergic activation by BF stimulation induces its effects only during the vibrotactile stimulus period. The significant effects on VS presented here are meaningful regarding vibrotactile stimulus period because of the mathematical definition of VS, but they do not exclude other effects which might be present throughout the experimental trials. For example, by obtaining single-unit and/or multi-unit data from multi-electrode recordings, other synchronicity measures (such as cross-correlations) may be studied within a population of neurons.

Regardless of BF stimulation, we have found that spontaneous activity of RS and FS neurons were different

especially in layer III, consistent with the previous literature. For example, layer and cell-type specific responses were reported in the rat barrel cortex with a trend towards higher response amplitudes in deeper layer II/III (de Kock et al. 2007; de Kock and Sakmann 2008). These studies have showed that spiking frequencies are very different and cell-type specific especially in layer V, but the related neurons were characterized as intrinsically bursting. It would also be interesting to analyze spike activity from simultaneous recordings from different cortical layers with BF stimulation; then, sensory processing in a columnar circuit can be better understood (Fox 2008).

Under anesthesia, it is very difficult to assess the characteristics or possible mechanisms of bottom-up and top-down attentional processes. BF (and NB) receives input from prefrontal cortex, and projects to posterior attention system and sensory areas as well as back to anterior attention system to process top-down signals (Sarter et al. 2005). It is rather complex to distinguish these signals. To understand their roles in somatosensory coding regarding hindpaw inputs requires very tedious behavioral experiments in which vibrotactile stimulus control is critical (Devecioğlu and Güçlü 2015, 2017; Öztürk et al. 2019). With this limitation in mind, we nevertheless attempted to mimic ‘top-down’ modulation of attention by applying electrical stimulation of BF just prior to the sensory input. The presented data can be compared with results from chronic stimulation/recording experiments in awake rats. We are currently working on a Bayesian model to track behavioral responses by multi-unit data. It would be interesting to study how the spike activity and the model change based on attentional shifts in psychophysical task or artificially by cholinergic activation by electrical or pharmacological means.

Although the current study cannot assess whether BF stimulation primarily activated nicotinic and/or muscarinic receptors, the preliminary data with nicotinic antagonists mentioned in the Results section and our previous work discussed here imply that the remaining effects observed through synchronization may be due to muscarinic receptor upregulation. Cholinergic receptor distributions are not homogeneous in the rat parietal cortex (Van Der Zee et al. 1992), and plastic changes can occur if the balance between nicotinic and muscarinic receptors is altered in cortical circuitry (Tian et al. 2011). The neurophysiological layer differences evidenced in the presented work may be related to the contribution of above two factors, i.e., particular distribution of different receptor types and plasticity induced by BF stimulation. However, because successive penetrations of our recording electrodes (multi-barrel pipette and carbon fiber combination electrode) typically damaged several cortical layers, we could not compare histological results

(e.g., obtained by antibodies against receptor proteins) and neurophysiological results in the same animals.

**Acknowledgements** This work was supported by Boğaziçi University Research Fund (BAP no. 17XP2) granted to Dr. Güçlü. We would like to thank Sevgi Öztürk and Begüm Devlet for help in the experiments.

**Funding** This study was funded by Boğaziçi University Research Fund (BAP no. 17XP2).

## Compliance with ethical standards

**Ethical approval** All procedures performed in studies involving animals were in accordance with the ethical standards of the institution or practice at which the studies were conducted (Boğaziçi University Institutional Ethics Committee for the Local Use of Animals in Experiments, 16.03.2017).

**Conflict of interest** The authors declare that they have no conflicts of interest.

## References

- Ahissar E, Sosnik R, Haidarliu S (2000) Transformation from temporal to rate coding in a somatosensory thalamocortical pathway. *Nature* 406:302–306. <https://doi.org/10.1038/35018568>
- Ballinger EC, Ananth M, Talmage DA et al (2016) Basal forebrain cholinergic circuits and signaling in cognition and cognitive decline. *Neuron* 91:1199–1218. <https://doi.org/10.1038/35018568>
- Burton H, Sinclair RJ, Hon SG et al (1997) Tactile-spatial and cross-modal attention effects in the second somatosensory and 7b cortical areas of rhesus monkeys. *Somatosens Mot Res* 14:237–267
- Castro-Alamancos MA (2004) Dynamics of sensory thalamocortical synaptic networks during information processing states. *Prog Neurobiol* 74:213–247. <https://doi.org/10.1016/j.pneurobio.2004.09.002>
- Castro-Alamancos MA, Bezdudnaya T, Deleuze C et al (2002) Properties of primary sensory (lemniscal) synapses in the ventrobasal thalamus and the relay of high-frequency sensory inputs. *J Neurophysiol* 87:946–953. <https://doi.org/10.1013/jphysiol.2001.013283>
- Chapin JK (1986) Laminar differences in sizes, shapes, and response profiles of cutaneous receptive fields in the rat SI cortex. *Exp Brain Res* 62:549–559. <https://doi.org/10.1007/BF00236033>
- Chapin JK, Lin CS (1984) Mapping the body representation in the SI cortex of anesthetized and awake rats. *J Comp Neurol* 229:199–213. <https://doi.org/10.1002/cne.902290206>
- Chapin JK, Sadeq M, Guise JL (1987) Corticocortical connections within the primary somatosensory cortex of the rat. *J Comp Neurol* 263:326–346. <https://doi.org/10.1002/cne.902630303>
- Chaves-Coira I, Martín-Cortecero J, Nuñez A, Rodrigo-Angulo ML (2018a) Basal forebrain nuclei display distinct projecting pathways and functional circuits to sensory primary and prefrontal cortices in the rat. *Front Neuroanat* 12:69. <https://doi.org/10.3389/fnana.2018.00069>
- Chaves-Coira I, Rodrigo-Angulo ML, Nuñez A (2018b) Bilateral pathways from the basal forebrain to sensory cortices may contribute to synchronous sensory processing. *Front Neuroanat* 12:5. <https://doi.org/10.3389/fnana.2018.00005>

- Cohen JC, Makous JC, Bolanowski SJ (1999) Under which conditions do the skin and probe decouple during sinusoidal vibrations? *Exp Brain Res* 129:211–217
- Connors BW, Gutnick MJ (1990) Intrinsic firing patterns of diverse neocortical neurons. *Trends Neurosci* 13:99–104
- Constantinople CM, Bruno RM (2011) Effects and mechanisms of wakefulness on local cortical networks. *Neuron*. <https://doi.org/10.1016/j.neuron.2011.02.040>
- De Kock CPJ, Sakmann B (2008) High frequency action potential bursts ( $\geq 100$  Hz) in L2/3 and L5B thick tufted neurons in anaesthetized and awake rat primary somatosensory cortex. *J Physiol* 586:3353–3364. <https://doi.org/10.1113/jphysiol.2008.155580>
- De Kock CPJ, Bruno RM, Spors H, Sakmann B (2007) Layer- and cell-type-specific suprathreshold stimulus representation in rat primary somatosensory cortex. *J Physiol* 581:139–154. <https://doi.org/10.1113/jphysiol.2006.124321>
- Devecioğlu I, Güçlü B (2013) Asymmetric response properties of rapidly adapting mechanoreceptive fibers in the rat glabrous skin. *Somatosens Mot Res* 30:16–29. <https://doi.org/10.3109/08990220.2012.732128>
- Devecioğlu I, Güçlü B (2015) A novel vibrotactile system for stimulating the glabrous skin of awake freely behaving rats during operant conditioning. *J Neurosci Methods* 242:41. <https://doi.org/10.1016/j.jneumeth.2015.01.004>
- Devecioğlu I, Güçlü B (2017) Psychophysical correspondence between vibrotactile intensity and intracortical microstimulation for tactile neuroprostheses in rats. *J Neural Eng*. <https://doi.org/10.1088/1741-2552/14/1/016010>
- Donoghue JP, Carroll KL (1987) Cholinergic modulation of sensory responses in rat primary somatic sensory cortex. *Brain Res* 408:367–371
- Dykes RWW, Lamour Y (1988) An electrophysiological study of single somatosensory neurons in rat granular cortex serving the limbs: a laminar analysis. *J Neurophysiol* 60:703–724. <https://doi.org/10.1038/10131>
- Everitt BJ, Robbins TW (1997) Central cholinergic systems and cognition. *Annu Rev Psychol* 48:649–684. <https://doi.org/10.1146/annurev.psych.48.1.649>
- Fiser J, Chiu C, Weliky M (2004) Small modulation of ongoing cortical dynamics by sensory input during natural vision. *Nature* 431:573–578. <https://doi.org/10.1038/nature02907>
- Foffani G, Tutunculer B, Moxon KA (2004) Role of spike timing in the forelimb somatosensory cortex of the rat. *J Neurosci* 24:7266–7271. <https://doi.org/10.1523/jneurosci.2523-04.2004>
- Fox K (2008) Barrel cortex. Cambridge University Press, Cambridge
- Froemke RC, Merzenich MM, Schreiner CE (2007) A synaptic memory trace for cortical receptive field plasticity. *Nature* 450:425–429. <https://doi.org/10.1038/nature06289>
- Gabernet L, Jadhav SP, Feldman DE et al (2005) Somatosensory integration controlled by dynamic thalamocortical feed-forward inhibition. *Neuron* 48:315–327. <https://doi.org/10.1016/j.neuron.2005.09.022>
- Gil Z, Amitai Y (1996) Adult thalamocortical transmission involves both NMDA and non-NMDA receptors. *J Neurophysiol* 76:2547–2553. <https://doi.org/10.1152/jn.1996.76.4.2547>
- Goard M, Dan Y (2009) Basal forebrain activation enhances cortical coding of natural scenes. *Nat Neurosci* 12:1444–1449. <https://doi.org/10.1038/nn.2402>
- Goodwin AW, Browning AS, Wheat HE (1995) Representation of curved surfaces in responses of mechanoreceptive afferent fibers innervating the monkey's fingerpad. *J Neurosci* 15:798–810
- Grün S, Rotter S (2010) Analysis of parallel spike trains. Springer, New York
- Güçlü B (2013) Vibrotactile responses of cortical neurons from hind-paw representation in the rat SI cortex. *Society for Neuroscience Abstracts*, 39, program no. 72.16
- Güçlü B, Bolanowski SJ (2003a) Frequency responses of cat rapidly adapting mechanoreceptive fibers. *Somatosens Mot Res* 20:249–263
- Güçlü B, Bolanowski SJ (2003b) Distribution of the intensity-characteristic parameters of cat rapidly adapting mechanoreceptive fibers. *Somatosens Mot Res* 20:149–155
- Güçlü B, Bolanowski SJ (2004) Tristate Markov model for the firing statistics of rapidly-adapting mechanoreceptive fibers. *J Comput Neurosci* 17:107–126
- Güçlü B, Bolanowski SJ, Pawson L (2003) End-to-end linkage (EEL) clustering algorithm: a study on the distribution of Meissner corpuscles in the skin. *J Comput Neurosci* 15:19–28. <https://doi.org/10.1023/A:1024466617694>
- Güçlü B, Mahoney GK, Pawson LJ et al (2008) Localization of Merkel cells in the monkey skin: an anatomical model. *Somatosens Mot Res* 25:123–138. <https://doi.org/10.1080/08990220802131234>
- Harris JA, Petersen RS, Diamond ME (1999) Distribution of tactile learning and its neural basis. *Proc Natl Acad Sci USA* 96:7587–7591
- Hasselmo ME, Schnell E, Barkai E (1995) Dynamics of learning and recall at excitatory recurrent synapses and cholinergic modulation in rat hippocampal region CA3. *J Neurosci* 15:5249–5262
- Henderson Z, Lu CB, Janzso G et al (2010) Distribution and role of Kv3.1b in neurons in the medial septum diagonal band complex. *Neuroscience* 166:952–969. <https://doi.org/10.1016/J.NEUROSCIENCE.2010.01.020>
- Henny P, Jones BE (2008) Projections from basal forebrain to prefrontal cortex comprise cholinergic, GABAergic and glutamatergic inputs to pyramidal cells or interneurons. *Eur J Neurosci* 27:654–670. <https://doi.org/10.1111/j.1460-9568.2008.06029.x>
- Herremans AHJ, Hijzen TH, Welborn PFE et al (1996) Effects of infusion of cholinergic drugs into the prefrontal cortex area on delayed matching to position performance in the rat. *Brain Res* 711:102–111. [https://doi.org/10.1016/0006-8993\(95\)01404-7](https://doi.org/10.1016/0006-8993(95)01404-7)
- Herrero JL, Roberts MJ, Delicato LS et al (2008) Acetylcholine contributes through muscarinic receptors to attentional modulation in V1. *Nature* 454:1110–1114. <https://doi.org/10.1038/nature07141>
- Himmelheber AM, Sarter M, Bruno JP (2000) Increases in cortical acetylcholine release during sustained attention performance in rats. *Cogn Brain Res* 9:313–325. [https://doi.org/10.1016/S0926-6410\(00\)00012-4](https://doi.org/10.1016/S0926-6410(00)00012-4)
- Himmelheber AM, Sarter M, Bruno JP (2001) The effects of manipulations of attentional demand on cortical acetylcholine release. *Cogn Brain Res* 12:353–370. [https://doi.org/10.1016/S0926-6410\(01\)00064-7](https://doi.org/10.1016/S0926-6410(01)00064-7)
- Hsiao SS, O'Shaughnessy DM, Johnson KO (1993) Effects of selective attention on spatial form processing in monkey primary and secondary somatosensory cortex. *J Neurophysiol* 70:444–447
- Hur EE, Zaborszky L (2005) Vglut2 afferents to the medial prefrontal and primary somatosensory cortices: a combined retrograde tracing in situ hybridization. *J Comp Neurol* 483:351–373. <https://doi.org/10.1002/cne.20444>
- Hyvärinen J, Poranen A, Jokinen Y (1980) Influence of attentive behavior on neuronal responses to vibration in primary somatosensory cortex of the monkey. *J Neurophysiol* 43:870–882
- Johansson RS, Landstrom U, Lundstrom R (1982) Responses of mechanoreceptive afferent units in the glabrous skin of the human hand to sinusoidal skin displacements. *Brain Res* 244:17–25
- Kilgard MP, Merzenich MM (1998) Cortical map reorganization enabled by nucleus basalis activity. *Science* 279:1714–1718. <https://doi.org/10.1126/science.279.5357.1714>
- Klinkenberg I, Sambeth A, Blokland A (2011) Acetylcholine and attention. *Behav Brain Res* 221:430–442. <https://doi.org/10.1016/j.bbr.2010.11.033>

- Kyriazi HT, Simons DJ (1993) Thalamocortical response transformations in simulated whisker barrels. *J Neurosci* 13:1601–1615
- Lamour Y, Dutar P, Jobert A, Dykes RW (1988) An iontophoretic study of single somatosensory neurons in rat granular cortex serving the limbs: a laminar analysis of glutamate and acetylcholine effects on receptive-field properties. *J Neurophysiol* 60:725–750
- Leem JW, Willis WD, Weller SC, Chung JM (1993) Differential activation and classification of cutaneous afferents in the rat. *J Neurophysiol* 70:2411–2424
- Levin ED, McClernon FJ, Rezvani AH (2006) Nicotinic effects on cognitive function: behavioral characterization, pharmacological specification, and anatomic localization. *Psychopharmacology* 184:523–539. <https://doi.org/10.1007/s00213-005-0164-7>
- Lin Y, Phillis JW (1991) Muscarinic agonist-mediated induction of long-term potentiation in rat cerebral cortex. *Brain Res* 551:342–345. [https://doi.org/10.1016/0006-8993\(91\)90955-U](https://doi.org/10.1016/0006-8993(91)90955-U)
- Martin-Cortecero J, Nuñez A (2014) Tactile response adaptation to whisker stimulation in the lemniscal somatosensory pathway of rats. *Brain Res* 1591:27–37. <https://doi.org/10.1016/j.brainres.2014.10.002>
- McKenna TM, Ashe JH, Hui GK, Weinberger NM (1988) Muscarinic agonists modulate spontaneous and evoked unit discharge in auditory cortex of cat. *Synapse* 2:54–68. <https://doi.org/10.1002/syn.890020109>
- Merrill DR, Bikson M, Jefferys JG (2005) Electrical stimulation of excitable tissue: design of efficacious and safe protocols. *J Neurosci Methods* 141:171–198. <https://doi.org/10.1016/j.jneumeth.2004.10.020>
- Mesulam MM, Mufson EJ, Wainer BH, Levey AI (1983) Central cholinergic pathways in the rat: an overview based on an alternative nomenclature (Ch1-Ch6). *Neuroscience* 10:1185–1201. [https://doi.org/10.1016/0306-4522\(83\)90108-2](https://doi.org/10.1016/0306-4522(83)90108-2)
- Metherate R, Ashe JH (1991) Basal forebrain stimulation modifies auditory cortex responsiveness by an action at muscarinic receptors. *Brain Res* 559:163–167
- Metherate R, Tremblay N, Dykes RW (1987) Acetylcholine permits long-term enhancement of neuronal responsiveness in cat primary somatosensory cortex. *Neuroscience* 22:75–81. [https://doi.org/10.1016/0306-4522\(87\)90198-9](https://doi.org/10.1016/0306-4522(87)90198-9)
- Metherate R, Tremblay N, Dykes RW (1988) The effects of acetylcholine on response properties of cat somatosensory cortical neurons. *J Neurophysiol* 59:1231–1252
- Minces V, Pinto L, Dan Y, Chiba AA (2017) Cholinergic shaping of neural correlations. *Proc Natl Acad Sci* 114:5725–5730. <https://doi.org/10.1073/pnas.1621493114>
- Mountcastle VB, Talbot WH, Sakata H, Hyvarinen J (1969) Cortical neuronal mechanisms in flutter-vibration studied in unanesthetized monkeys. Neuronal periodicity and frequency discrimination. *J Neurophysiol* 32:452–484
- Oldford E, Castro-Alamancos MA (2003) Input-specific effects of acetylcholine on sensory and intracortical evoked responses in the “barrel cortex” in vivo. *Neuroscience* 117:769–778. [https://doi.org/10.1016/S0306-4522\(02\)00663-2](https://doi.org/10.1016/S0306-4522(02)00663-2)
- Öztürk S, Devecioğlu I, Beygi M et al (2019) Real-time performance of a tactile neuroprosthesis on awake behaving rats. *IEEE Trans Neural Syst Rehabil Eng* 27:1053–1062. <https://doi.org/10.1109/TNSRE.2019.2910320>
- Paxinos G, Watson C (1997) The rat brain in stereotaxic coordinates, 3rd edn. Academic Press, San Diego
- Perry E, Walker M, Grace J, Perry R (1999) Acetylcholine in mind: a neurotransmitter correlate of consciousness? *Trends Neurosci* 22:273–280. [https://doi.org/10.1016/S0166-2236\(98\)01361-7](https://doi.org/10.1016/S0166-2236(98)01361-7)
- Picciotto MR, Higley MJ, Mineur YS (2012) Acetylcholine as a neuromodulator: cholinergic signaling shapes nervous system function and behavior. *Neuron* 76:116–129. <https://doi.org/10.1016/j.neuron.2012.08.036>
- Pinto DJ, Brumberg JC, Simons DJ (2000) Circuit dynamics and coding strategies in rodent somatosensory cortex. *J Neurophysiol* 83:1158–1166
- Pinto L, Goard MJ, Estandian D et al (2013) Fast modulation of visual perception by basal forebrain cholinergic neurons. *Nat Neurosci* 16:1857–1863. <https://doi.org/10.1038/nn.3552>
- Poranen A, Hyvarinen J (1982) Effects of attention on multiunit responses to vibration in the somatosensory regions of the monkey's brain. *Electroencephalogr Clin Neurophysiol* 53:525–537
- Porter JT, Johnson CK, Agmon A (2001) Diverse types of interneurons generate thalamus-evoked feedforward inhibition in the mouse barrel cortex. *J Neurosci* 21:2699–2710 (pii:21/8/2699)
- Poulet JFA, Petersen CCH (2008) Internal brain state regulates membrane potential synchrony in barrel cortex of behaving mice. *Nature* 454:881–885. <https://doi.org/10.1038/nature07150>
- Rasmusson DD, Dykes RW (1988) Long-term enhancement of evoked potentials in cat somatosensory cortex produced by co-activation of the basal forebrain and cutaneous receptors. *Exp Brain Res* 70:276–286
- Richardson RT, DeLong MR (1986) Nucleus basalis of Meynert neuronal activity during a delayed response task in monkey. *Brain Res* 399:364–368. [https://doi.org/10.1016/0006-8993\(86\)91529-5](https://doi.org/10.1016/0006-8993(86)91529-5)
- Sarter M, Hasselmo ME, Bruno JP, Givens B (2005) Unraveling the attentional functions of cortical cholinergic inputs: interactions between signal-driven and cognitive modulation of signal detection. *Brain Res Rev* 48:98–111. <https://doi.org/10.1016/j.brainresrev.2004.08.006>
- Sato H, Hata Y, Masui H, Tsumoto T (1987) A functional role of cholinergic innervation to neurons in the cat visual cortex. *J Neurophysiol* 58:765–780
- Semba K (2000) Multiple output pathways of the basal forebrain: organization, chemical heterogeneity, and roles in vigilance. *Behav Brain Res* 115:117–141. [https://doi.org/10.1016/S0166-4328\(00\)00254-0](https://doi.org/10.1016/S0166-4328(00)00254-0)
- Sillito AM, Kemp JA (1983) Cholinergic modulation of the functional organization of the cat visual cortex. *Brain Res* 289:143–155
- Simons DJ (1978) Response properties of vibrissa units in rat SI somatosensory neocortex. *J Neurophysiol* 41:798–820
- Steinmetz PN, Roy A, Fitzgerald PJ et al (2000) Attention modulates synchronized neuronal firing in primate somatosensory cortex. *Nature* 404:187–190. <https://doi.org/10.1038/35004588>
- Talbot WH, Darian-Smith I, Kornhuber HH, Mountcastle VB (1968) The sense of flutter-vibration: comparison of the human capacity with response patterns of mechanoreceptive afferents from the monkey hand. *J Neurophysiol* 31:301–334
- Tian MK, Bailey CD, De Biasi M et al (2011) Plasticity of prefrontal attention circuitry: upregulated muscarinic excitability in response to decreased nicotinic signaling following deletion of  $\alpha 5$  or  $\beta 2$  subunits. *J Neurosci* 31:16458–16463
- Torres EM, Perry TA, Blockland A et al (1994) Behavioural, histochemical and biochemical consequences of selective immunolesions in discrete regions of the basal forebrain cholinergic system. *Neuroscience* 63:95–122. [https://doi.org/10.1016/0306-4522\(94\)90010-8](https://doi.org/10.1016/0306-4522(94)90010-8)
- Tremblay N, Warren RA, Dykes RW (1990a) Electrophysiological studies of acetylcholine and the role of the basal forebrain in the somatosensory cortex of the cat. II. Cortical neurons excited by somatic stimuli. *J Neurophysiol* 64:1212–1222
- Tremblay N, Warren RA, Dykes RW (1990b) Electrophysiological studies of acetylcholine and the role of the basal forebrain in the somatosensory cortex of the cat. I. Cortical neurons excited by glutamate. *J Neurophysiol* 64:1199–1211
- Tsodyks M, Kenet T, Grinvald A, Arieli A (1999) Linking spontaneous activity of single cortical neurons and the underlying functional

- architecture. *Science* 286:1943–1946. <https://doi.org/10.1126/science.286.5446.1943>
- Tutunculer B, Foffani G, Himes BT, Moxon KA (2006) Structure of the excitatory receptive fields of infragranular forelimb neurons in the rat primary somatosensory cortex responding to touch. *Cereb Cortex* 16:791–810. <https://doi.org/10.1093/cercor/bhj023>
- Vahle-Hinz C, Detsch O, Siemers M, Kochs E (2007) Contributions of GABAergic and glutamatergic mechanisms to isoflurane-induced suppression of thalamic somatosensory information transfer. *Exp Brain Res* 176:159–172. <https://doi.org/10.1007/s00221-006-0604-6>
- Van Der Zee A, Streefland C, Strosberg AD et al (1992) Visualization of cholinceptive neurons in the rat neocortex: colocalization of muscarinic and nicotinic acetylcholine receptors. *Mol Brain Res* 14:326–336
- Vardar B, Güçlü B (2016) Differential effects of acetylcholine and atropine on vibrotactile responses of neurons in the hindpaw representation of rat SI cortex. *Anat Int J Exp Clin Anat* 10(1):O-20
- Vardar B, Güçlü B (2017) Non-NMDA receptor-mediated vibrotactile responses of neurons from the hindpaw representation in the rat SI cortex. *Somatosens Mot Res* 34:189–203. <https://doi.org/10.1080/08990220.2017.1390450>
- Vardar B, Güçlü B (2018) Basal forebrain stimulation modulates vibrotactile responses of rat SI neurons based on cell type, layer, and in a time-dependent manner. *Society for Neuroscience Abstracts*, 44, program no. 392.03
- Vega-Bermudez F, Johnson KO (1999) SA1 and RA receptive fields, response variability, and population responses mapped with a probe array. *J Neurophysiol* 81:2701–2710
- Verdier D, Dykes RW (2001) Long-term cholinergic enhancement of evoked potentials in rat hindlimb somatosensory cortex displays characteristics of long-term potentiation. *Exp Brain Res* 137:71–82. <https://doi.org/10.1007/s002210000646>
- Welker C, Woolsey TA (1974) Structure of layer IV in the somatosensory neocortex of the rat: description and comparison with the mouse. *J Comp Neurol* 158:437–453. <https://doi.org/10.1002/cne.901580405>
- Whitsel BL, Kelly EF, Delemos KA et al (2000) Stability of rapidly adapting afferent entrainment vs responsiveness. *Somatosens Mot Res* 17:13–31
- Yusufogullari S, Kılınç D, Vardar B et al (2015) Sıçanda farklı korteks alanlarındaki katman kalınlıklarının histolojik olarak incelenmesi. In: Usta A (ed) BİYOMUT 2015, proceedings of 19th national biomedical engineering meeting, İstanbul, Turkey, no: S12
- Záborszky L, Heimer L, Eckenstein F, Leranth C (1986) GABAergic input to cholinergic forebrain neurons: an ultrastructural study using retrograde tracing of HRP and double immunolabeling. *J Comp Neurol* 250:282–295. <https://doi.org/10.1002/cne.902500303>
- Záborszky L, Pang K, Somogyi J et al (1999) The basal forebrain corticopetal system revisited. *Ann N Y Acad Sci* 877:339–367. <https://doi.org/10.1111/j.1749-6632.1999.tb09276.x>
- Záborszky L, van den Pol AN, Gyengesi E (2012) The basal forebrain cholinergic projection system in mice. In: *The mouse nervous system*. Academic Press, Cambridge, pp 684–718
- Záborszky L, Csordas A, Mosca K et al (2015) Neurons in the basal forebrain project to the cortex in a complex topographic organization that reflects corticocortical connectivity patterns: an experimental study based on retrograde tracing and 3D reconstruction. *Cereb Cortex* 25:118–137. <https://doi.org/10.1093/cercor/bht210>
- Záborszky L, Gombkoto P, Varsanyi P et al (2018) Specific basal forebrain-cortical cholinergic circuits coordinate cognitive operations. *J Neurosci* 38:9446–9458. <https://doi.org/10.1523/JNEUROSCI.1676-18.2018>

**Publisher's Note** Springer Nature remains neutral with regard to jurisdictional claims in published maps and institutional affiliations.